Computer-Aided Detection of Colonic Polyps using Volume Rendering

Wei Hong, Feng Qiu, Joseph Marino, Arie Kaufman
Center for Visual Computing and Department of Computer Science
Stony Brook University, Stony Brook, NY 11794-4400

ABSTRACT

This work utilizes a novel pipeline for the computer-aided detection (CAD) of colonic polyps, assisting radiologists in locating polyps when using a virtual colonoscopy system. Our CAD pipeline automatically detects polyps while reducing the number of false positives (FPs). It integrates volume rendering and conformal colon flattening with texture and shape analysis. The colon is first digitally cleansed, segmented, and extracted from the CT dataset of the abdomen. The colon surface is then mapped to a 2D rectangle using conformal mapping. Using this colon flattening method, the CAD problem is converted from 3D into 2D. The flattened image is rendered using a direct volume rendering of the 3D colon dataset with a translucent transfer function. Suspicious polyps are detected by applying a clustering method on the 2D volume rendered image. The FPs are reduced by analyzing shape and texture features of the suspicious areas detected by the clustering step. Compared with shape-based methods, ours is much faster and much more efficient as it avoids computing curvature and other shape parameters for the whole colon wall. We tested our method with 178 datasets and found it to be 100% sensitive to adenomatous polyps with a low rate of FPs. The CAD results are seamlessly integrated into a virtual colonoscopy system, providing the radiologists with visual cues and likelihood indicators of areas likely to contain polyps, and allowing them to quickly inspect the suspicious areas and further exploit the flattened colon view for easy navigation and bookmark placement.

Keywords: Computer-Aided Detection, CAD, Virtual Colonoscopy, Texture Analysis, Conformal Colon Flattening

1. INTRODUCTION

The second leading cause of cancer-related deaths in the United States is colorectal cancer. It is recommended that adults should be screened to detect cancer-related polyps. The traditional screening using *optical colonoscopy* (OC), however, is invasive, expensive, time-consuming, incomplete, uncomfortable, and requires an intensive bowel preparation. Because of this, many are not screened. *Virtual colonoscopy* (VC), also known as *computed tomogrpahic colonography* (CTC), has been developed to help encourage adults to be regularly screened for polyps [9, 12, 19]. Unlike the OC, VC does not require the insertion of a colonoscope or sedation. Rather, the patient undergoes a breath-hold *computed tomography* (CT) scan, from which the computer generates a 3D model of the patient's colon that is used by the radiologist to navigate inside of it in search of polyps. The VC also doesn't require a rigorous bowel cleansing preparation. The computer is able to electronically cleanse the colon. The patient needs only have a modified diet with an oral contrast agent.

For a radiologist to make an accurate determination about the existence of polyps utilizing a virtual colonoscopy system, it is necessary for her/him to spend a substantial amount of time carefully inspecting the entire colon wall during navigation. Even with a careful inspection, it is easy for the radiologist to miss polyps that might be hidden around sharp bends and within deep folds of the colon wall. A *computer-aided detection* (CAD) system can help in this process by pointing out to the radiologist areas of interest that need more specific attention. This assures the radiologists that they inspect these critical locations. In order for the CAD system to be useful, it must be able to identify 100% of the polyps. In addition, it must be able to substantially reduce the number of FPs. Without the reduction of FPs, there would be too many areas to be inspected in a limited amount of time. An efficient CAD system would thus be used to make radiologists more effective and make their diagnoses more accurate.

In the past several years there have been several prototype CAD schemes reported in the literature with variable success of polyp detection. Shape features are the major mechanisms that have been used to differentiate polyps from normal tissues [16, 18, 20, 21, 22, 25, 29]. All of these shape based methods are sensitive to the irregularity of the colon wall and therefore share a relatively high FP rate, which is undesirable. Thus, many methods [1, 17, 27] have been studied to

Medical Imaging 2007: Computer-Aided Diagnosis, edited by Maryellen L. Giger, Nico Karssemeijer,
Proc. of SPIE Vol. 6514, 651406, (2007) · 1605-7422/07/$18 · doi: 10.1117/12.710022

further reduce false positives. In our method, we conformally map the colon surface to a 2D rectangle, which simplifies the polyp detection problem from 3D to 2D, detect polyps using volume rendering of the 3D colon dataset, which is a texture-based method, and reduce FPs using shape and texture features.

2. METHOD

Previous research has shown differences between the internal tissue of polyps and healthy tissue. It has been observed that the density of the internal tissues of polyps is higher that that of healthy tissues. It has also been observed that there is a difference in the textures of these tissues. These high density areas cannot be seen in an optical colonoscopy because they are located beneath the colon wall. Volume rendering of the virtual data with a translucent transfer function can, however, reveal the internal structure of polyps [23], as shown in Figure 1. This is called *electronic biopsy*. In the electronic biopsy image (Figure 1(b)), the red color represents the highest densities, blue represents the lowest densities, and green represents tissues of middle densities. The idea for this work is that polyps can be detected by analyzing the electronic biopsy images of the entire colon, based on the observations about polyp tissue density.

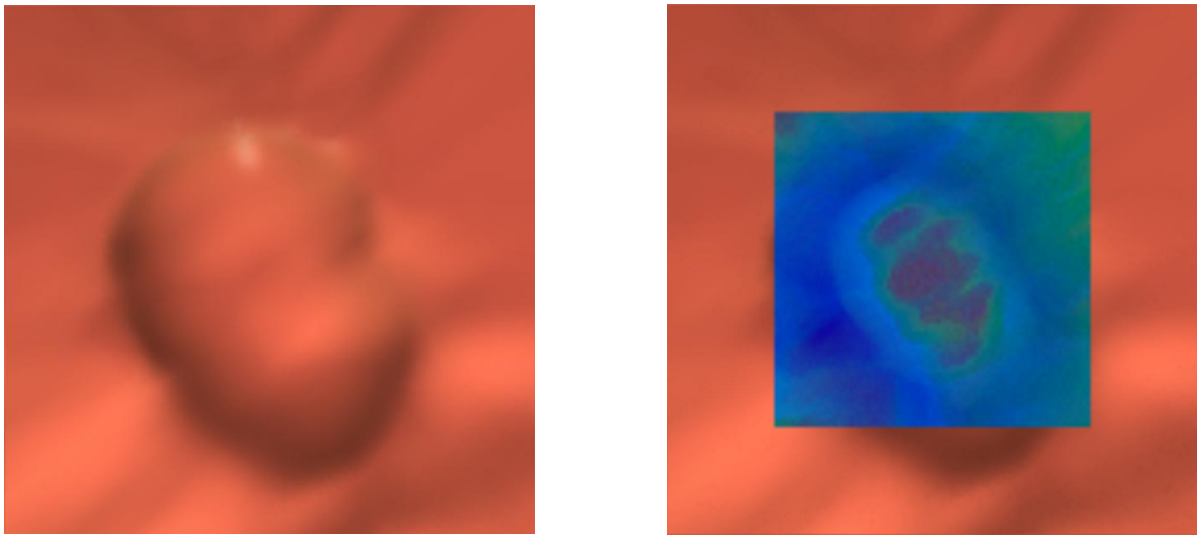

(a) (b)

Figure 1. Electronic biopsy: (a) Surface rendering of an adenomatous polyp; (b) the electronic biopsy rendering of the polyp.

A diagram of our CAD pipeline is shown in Figure 2. First, for segmentation and digital cleansing of the colon, an iterative partial volume segmentation algorithm is applied. Then, a colon surface is extracted followed by conformal colon flattening. The electronic biopsy colon image is then generated using a volumetric ray casting algorithm on the entire flattened colon. After that, our clustering algorithm and reduction of FPs are performed. All of these processes are performed automatically in our pipeline. The details of each step are discussed in the following subsections, and further details can be found in [11].

2.1 Segmentation and digital cleansing

The first step in our pipeline is to segment the colon lumen from the CT scan of the patient's abdomen. The day prior to the scan, the patient drinks an oral contrast agent (i.e., barium) in order to tag colonic material, making it unnecessary for the colon to be cleansed physically. The tagged material is clearly visible in the CT scan, allowing it to be identified. Care must be taken during electronic cleansing to restore CT density values where the partial-volume effect occurs.

Once the colon has been electronically cleansed, we can obtain a segmentation of the colon and a clean colon lumen. We use a statistical method for colon segmentation to handle the partial volume effect. Instead of labeling each voxel with a unique class type, the percentage of different material classes are estimated within each voxel [26]. We model each voxel as a sum of participating pure tissue components. The observed density value at voxel i is expressed as y_i:

$$y_i = \sum_{k=1}^{n} m_{ik}\mu_k + \varepsilon_i, \quad \sum_{k=1}^{n} m_{ik} = 1 \text{ and } 0 \le m_{ik} \le 1 \tag{1}$$

where ε_i is Gaussian noise associated with y_i at voxel i with its mean being zero, m_{ik} is called the mixture which represents the contribution of class type k to this voxel i, and μ_k is the mean of class type k. Our goal is to determine the tissue mixtures and the parameters of the Gaussian models. The well developed expectation-maximization algorithm (EM algorithm) is used to estimate these parameters in an iterative manner. When we obtain the mixture information within each voxel, a voxel can be classified as air, soft tissue, or bone if one of its mixtures is larger than a threshold, say 95%. If a voxel has two major classes, it has partial volume effect, and it can be classified as the boundary of these two classes. In Figure 3(c), we show the classification result for one CT image, in which air is shown in red, soft tissue is shown in green, bone and tagged material are shown in blue, and the interface between air and tagged material is shown in pink.

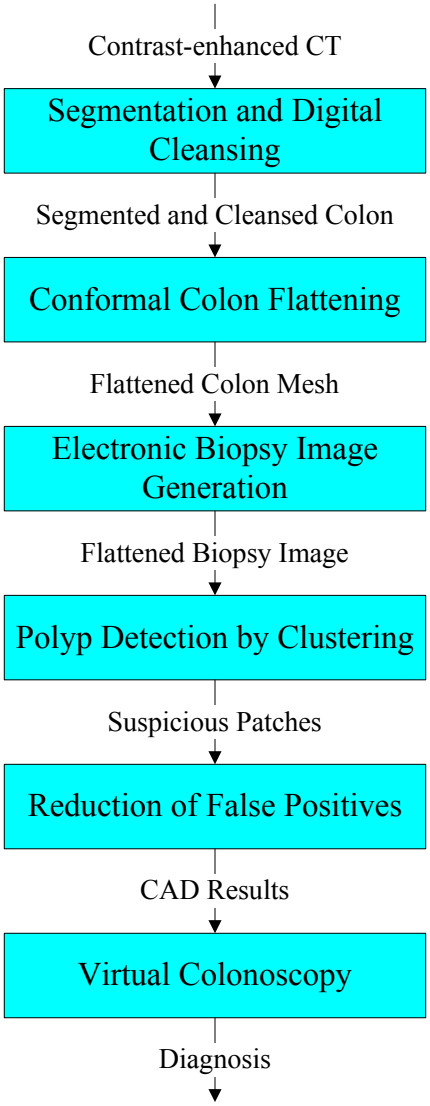

Figure 2. Our CAD pipeline.

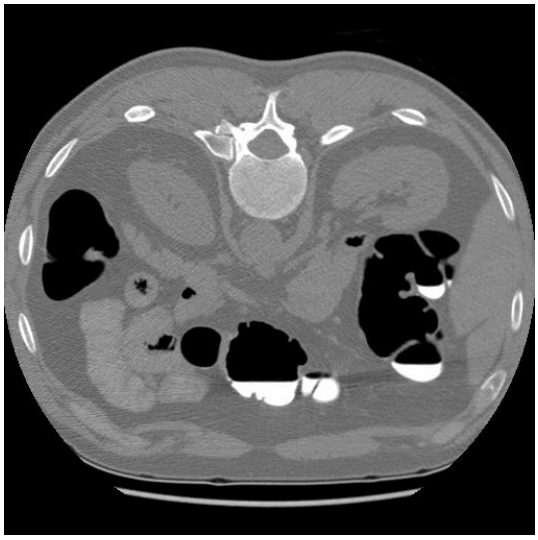

(a) An original CT image

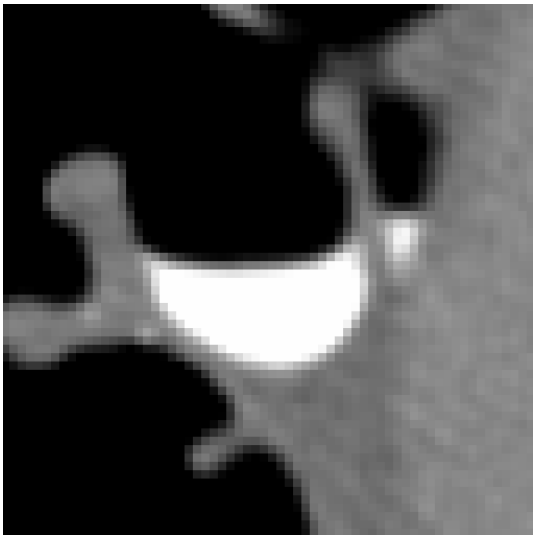

(b) A zoomed-in view of (a)

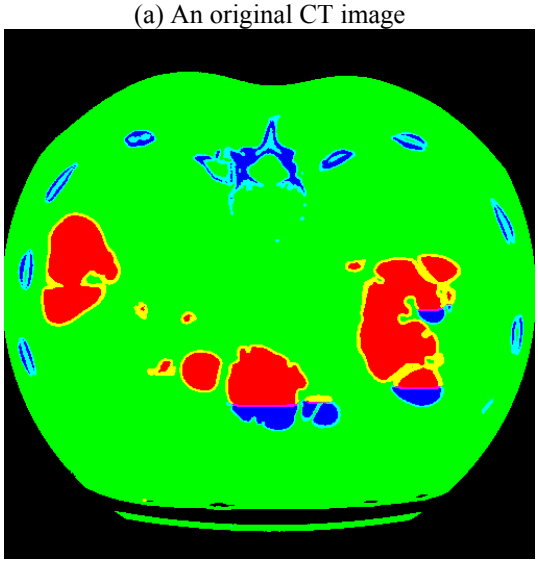

(c) Classification result

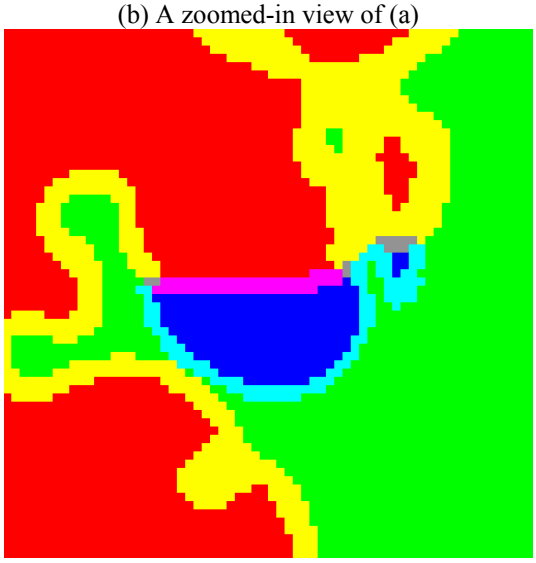

(d) A zoomed-in view of (c)

Figure 3: Automatic colon segmentation.

After classification, we need to segment the colon lumen. The voxels in the colon lumen are classified as air, mixture of air with tissue, mixture of air with tagged materials, or mixture of tissue with tagged materials. First, we use a labeling algorithm to extract all connected components for the whole dataset. It is noted that the interface layers between air and tagged fluid should be flat, and must be below its neighboring air component and above its neighboring tagged material component due to gravity. Therefore, we first identify these interface layers and mark them as colon. Then, the air and fluid components connected with these interface layers are also marked as colon.

When we obtained the segmentation of the colon lumen, the tagged material within the colon lumen is cleansed based on Equation 2. The idea is that we can remove the contribution of fluid and add some contribution of air or soft tissue using the mixture information. The equation to remove the tagged material is expressed as in Equation 2.

$$y_{new} = y_{old} - m_{tag}\mu_{tag} + m_{air}\mu_{air} \tag{2}$$

The enhanced mucosa layer can also be restored using a similar equation.

2.2 Conformal colon flattening

Once the CT scan has been segmented and cleansed digitally, it is necessary to extract the surface of the colon. The results from this step are both the extracted 3D colon surface mesh and the flattened colon mesh. The colon surface is extracted through a topology-preserving dual contouring method [30] using the segmented colon.

In the 3D endoscopic view of the virtual colonoscopy system, we can only see a small part of the colon. Moreover, our views are blocked by the colon haustral folds, and therefore many regions will not be visible in the endoscopic view. The worst scenario is that polyps are not visible and may be missed during navigation. Virtual colon flattening is an efficient visualization technique for polyp detection, in which the entire inner surface of the colon is displayed as a single 2D image. However, if two surfaces do not have the same Gaussian curvature, there does not exist a mapping which achieves both area and angle preservation. Several methods have been developed that are either area preserving [3] or angle preserving [7]. Our method [10] is also angle preserving, and thus the rounded shape information of the polyps is preserved in the flattened view. This is useful for the radiologists, who identify polyps mainly based on their shape. Unlike Haker et al.'s method [7] that maps the colon surface to a parallelogram, we map the colon surface to a 2D rectangle.

Instead of directly computing the conformal map between the 3D colon surface and a 2D rectangle, we compute its gradient field first. Mathematically, this gradient field is called holomorphic 1-form. Then, the conformal mapping can be obtained by integration. Each gradient field of a conformal map is a pair of tangential vector fields with special properties, such that the curl and Laplace are zero everywhere. All such vector fields form a linear space. We construct a basis of this linear space by solving a linear system derived from these properties. The global distortion from the colon surface to the parametric rectangle is minimized, which is measured by harmonic energy. The details of our flattening algorithm can be found in [10].

As postulated in previous CAD papers [28, 29], the colonic polyps usually have an elliptic curvature of the peak subtype, i.e., the shape at the top section of a regular polyp (toward the colon lumen) is more likely to be a spherical cap. Because of the angle preservation of our colon flattening algorithm, the elliptic shape of a colonic polyp is preserved in the flattened image. It is noted that our conformal colon flattening has area distortion, yet minimizes the global distortion. Consequently, polyps cannot be directly measured on the 2D flattened colon image. Since we maintain a one-to-one mapping between the 3D vertices and 2D vertices of the colon mesh, polyps can still be measured in 3D. Geometric features and texture features can also be computed in 3D and mapped to 2D. This conformal mapping substantially simplifies our polyp detection problem from 3D to 2D.

2.3 Electronic biopsy image generation

In this step, a 2D electronic biopsy image of the entire flattened colon wall is generated, which captures the information that is inside of the colon wall. Each voxel is assigned a color and opaqueness based on its CT density. A volumetric ray-casting algorithm is performed for each pixel in the 2D flattened image. When the ray enters the volume, it accumulates the color and opacity values of the voxels that is passes through. We use a sampling distance of 0.5 mm and limit the ray to a traversal of 40 steps because we are interested only in the thin layer (20 mm or so) beneath the colon surface. The rays are also terminated if they re-enter the colon lumen (for example, by passing through a wall in the colon that protrudes into the lumen, such as a fold). We can efficiently generate high resolution electronic biopsy images accelerated on the GPU [11, 14], where the thin layer beneath the colon wall is even super-sampled. An electronic biopsy image of a flattened colon is shown in Figure 4.

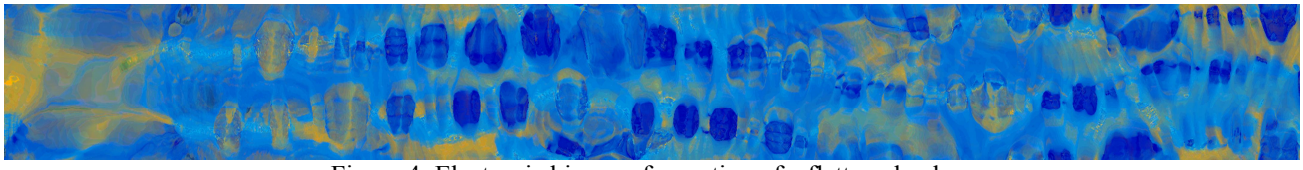

Figure 4: Electronic biopsy of a portion of a flattened colon.

2.4 Polyp detection by clustering

It is observed that similar color features appear in contiguous areas in several regions of the 2D electronic biopsy image. Clustering is performed on the 2D electronic biopsy image for polyp detection. It classifies regions with similar color features. After running the clustering algorithm, pixels that are classified as belonging to a polyp are marked as such. We then extract the suspicious polyps with a connected-component algorithm. Since we only consider the polyps with a diameter larger than 5mm, a component whose size is below such a threshold is classified as a false-positive finding. Consequently, many suspicious regions with a diameter below 5mm are removed.

2.5 Reduction of false positives

To further reduce the number of FPs, we look at additional features, such as shape index and curvedness and volumetric texture features. The shape index is a measure of shape, and the curvedness measures the shape of the local neighborhood of a voxel. The different structures of the colon have different 3D shape information, and thus can be identified using the shape features. The colon wall itself is generally flat and cup-like, with small curvedness. The colon folds are generally large, ridge-like structures, with large curvedness. Polyps are generally bulbous structures, with small to medium curvedness. Furthermore, for a polyp, density gradient vectors tend to point towards the center. This can also be used to reduce FPs. Our pipeline computes these features only for suspicious areas for FP reduction, and not for the entire colon. Since the computation of these features is time consuming, limiting the computation to only the suspicious areas greatly improves the running time of our pipeline.

2.6 Integration with virtual colonoscopy

The results of our CAD pipeline have been integrated into a VC system. This integration allows the radiologist to focus on the regions that have been identified by our pipeline as being suspicious. This feature allows a second set of eyes to view the data, so that any suspiciously labeled areas will be doubly checked by the radiologist.

Our VC user interface shown in Figure 5 is interactive and provides many views of the colon. In the center is the 3D volume rendered endoscopic view of the virtual colon. The radiologist is able to fly through this virtual colon along the centerline and inspect the walls, stopping and changing views as necessary. This is most similar to a traditional OC. Unlike a traditional OC, the radiologist can fly-through the colon from both directions, so as to make sure that nothing is hiding on the other side of a fold. On the right side of our user interface are the original and reconstructed CT scan slices of the colon data. The slices are mutually perpendicular, and show the axial, sagittal, and coronal views of the colon data. To the left of the endoscopic view is an overview of the 3D reconstructed colon. This allows the radiologists an overview and the context as well as a mechanism for placing bookmarks for later reference. Below the 3D overview is a cross-sectional view in front of the user's eye perpendicular to the centerline. At the leftmost side is the flattened colon image created earlier in our pipeline. This provides a dissected view of the colon, which can be useful for an overview of the entire colon in one image. Since this image was created conformally, it is shape-preserving, and thus the shape of polyps will be easily identifiable to a radiologist on this image. The current position is marked and synchronized in all the different views, which are inter-linked.

The results of our CAD pipeline have also been integrated in other ways into a VC system, to make it as easy as possible for the radiologist to utilize these results. The suspicious areas are highlighted in the endoscopic view during navigation, in order to attract the attention of the radiologist using the system. Since our system is 100% sensitive to polyps, polyps that might have been missed by the radiologist in the conventional VC system will probably not be missed in ours. The suspicious areas are also highlighted on the 2D flattened image and the 3D overview. To inspect these regions in the endoscopic view, the radiologist needs only to click on these areas in the flattened image. All other linked views will be updated for viewing such an area. Our system also allows the radiologist to place bookmarks for any areas considered suspicious. These bookmarks are stored on both the flattened 2D image and the 3D overview of the colon. Clicking on a bookmark in either view will update all other views for better inspection of that area. Bookmarks for the areas found suspicious by our system are automatically provided.

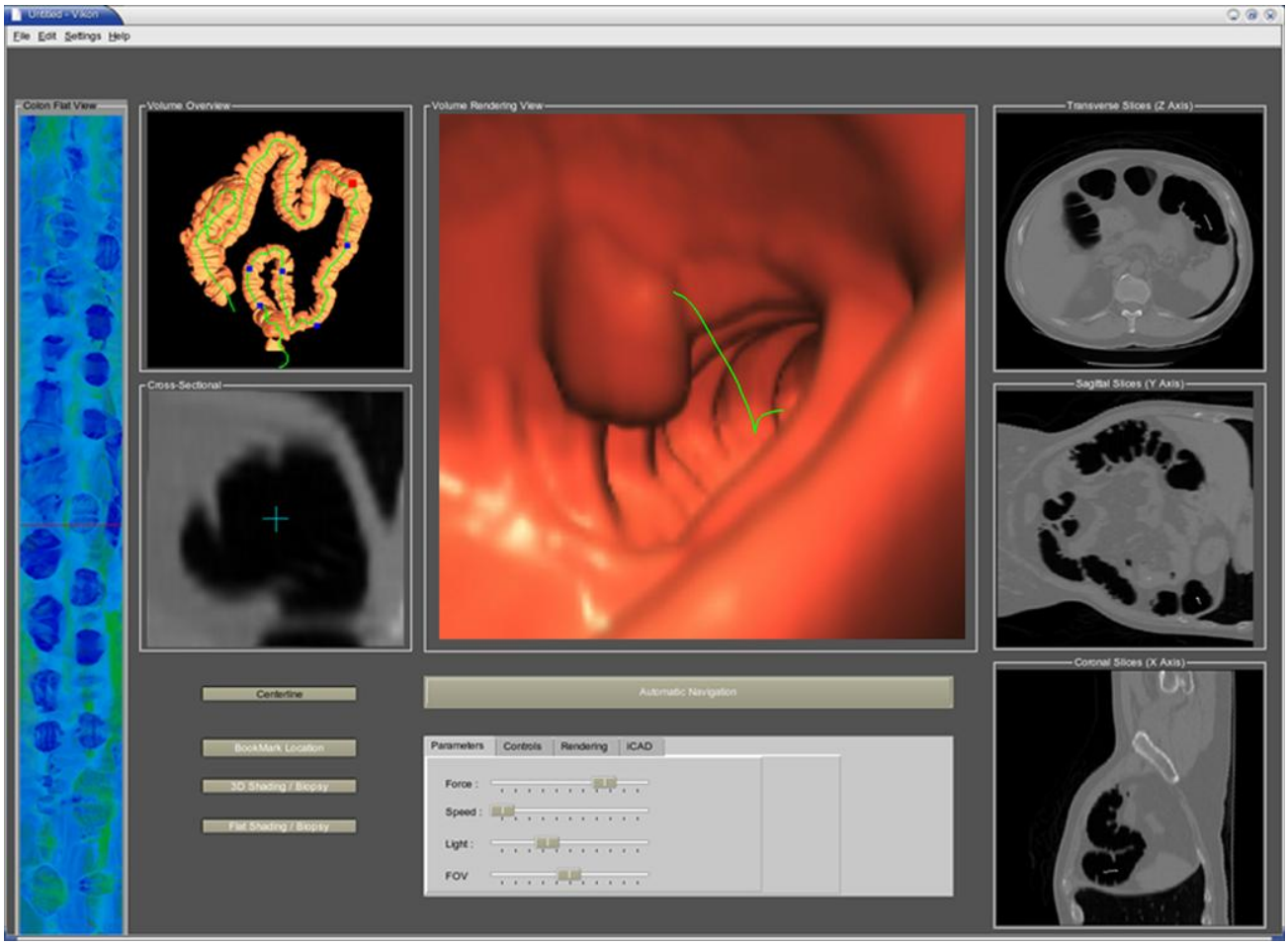

Figure 5: The user interface of our CAD system.

3. RESULTS

Our pipeline was tested using a total of 198 CT data sets. We used 152 CT data sets from the National Institute of Health (NIH) and 46 CT data sets from Stony Brook University Hospital (SBUH). The NIH data sets include, in addition to the raw DICOM images, VC reports, OC reports, pathology reports, and OC videos. The SBUH data sets include, in addition to the raw DICOM images, VC reports and OC reports. The reports included with each data set were used to confirm the results of our system.

Twenty data sets from the NIH were used in the training of our pipeline. The remaining 178 data sets were used to test our CAD pipeline. Our pipeline generated consistent results and is 100% sensitive to polyps. No polyp in the 132 NIH data sets or the 46 SBUH data sets used for testing was missed by our system. The results of testing our pipeline are depicted in Table 1.

Table 1. Experimental results of our CAD pipeline.

Data Source	Total Polyps	FP per Data Set	FP Reduction
SBUH	65	2.9	97.1%
NIH	82	3.5	96.1%

In addition to detecting all polyps, our pipeline also significantly reduced the number of FPs for each data set. The 132 NIH data sets used for testing contain 82 polyps, all of which were identified by our pipeline. An average of 3.5 FPs was

identified in each data set, after FP reduction. The FP reduction step removed 96.1% of the FPs. The 46 SBUH data sets contained 65 polyps, all of which were identified by our pipeline. An average of 2.9 FPs was identified in each data set, after FP reduction. The FP reduction step removed 97.1% of the FPs.

The best systems based on shape analysis achieved 100% sensitivity with 2 – 3 FPs per dataset. Our experimental results show that our system achieves similar results. Our system, though, is much faster when compared to shape-based CAD methods. We ran our system on a 3.6 GHz Pentium 4 PC running Windows XP with 3G RAM and an NVIDIA Quadro 4500 graphics card. The conformal colon flattening is the most time consuming step of our pipeline, which takes about seven minutes. Our pipeline takes in total about 16 minutes to extract the colon surface, flatten it, render an electronic biopsy image, and gather features for polyp detection. In contrast, using a purely shape-based method, the computation of shape index and curvedness is the most time consuming step. This step required about 20 minutes when using a mask size of 5 x 5 x 5 and about one hour when using a mask size of 7 x 7 x 7. This was tested using the same datasets and computer platform as was used to test our pipeline. It is also much easier to integrate our results into a VC system than the results from other systems because our results are stored in a 2D image.

4. CONCLUSIONS

The pipeline we present here is a novel method for the CAD of polyps. Unlike previous shape-based methods, our method uses a 2D volume rendered flattened biopsy image of the colon to detect suspicious patches by 2D clustering. FPs are reduced by performing shape analysis and 3D texture analysis only on these patches, not on the entire endoluminal colon surface. Our system detects 100% of the adenomatous polyps, and yields a low FP rate in only several minutes. The results are easily integrated into a VC system, which allows radiologists to perform their diagnoses more accurately and efficiently. Since the suspicious areas are clearly identified to the user, the radiologist needs only traverse the colon in one direction, without fear of missing a polyp.

In the future, we plan to study the registration of supine and prone scans for a VC patient, based on our conformal colon flattening technique. Results from this registration could be used to double check for polyp detection. We also plan to further reduce FPs with more advanced pattern recognition techniques.

ACKNOWLEDGEMENTS

This work has been partially supported by NSF grant CCR-0306438 and NIH grants CA082402 and CA110186. We disclose that one of the authors owns a fraction of Viatronix Inc. shares. We are grateful to the laboratory for imaging research and informatics (IRIS) at Stony Brook and its director Zhengrong Liang for the use of their partial volume segmentation code [26]. The CT colon datasets are courtesy of the National Institute of Health and Stony Brook University Hospital.

REFERENCES

1. B. Acar, C. Beaulieu, S. Gokturk, C. Tomasi, D. Paik, R. B. Jeffrey, J. Yee, and S. Napel. Edge displacement field-based classification for improved detection of polyps in CT colonography. *IEEE Transactions on Medical Imaging*, 21:1461–1467, 2002.
2. R. S. Avila, L. M. Sobierajski, and A. E. Kaufman. Towards a comprehensive volume visualization system. *IEEE Visualization*, pages 13–20, 1992.
3. A. V. Bartroli, R. Wegenkittl, A. Konig, and E. Groller. Nonlinear virtual colon unfolding. *IEEE Visualization*, pages 411–418, Oct. 2001.
4. G. Bertrand. Simple points, topological numbers and geodesic neighborhoods in cubic grids. *Pattern Recognition Letters*, 15:1003–1011, 1994.
5. B. Cabral, N. Cam, and J. Foran. Accelerated volume rendering and tomographic reconstruction using texture mapping hardware. *Symposium on Volume Visualization*, pages 91–98, 1994.
6. S. B. Göktürk, C. Tomasi, B. Acar, C. F. Beaulieu, D. S. Paik, R. B. Jeffrey, J. Yee, and S. Napel. A statistical 3D pattern processing method for computer aided detection of polyps in CT colonography. *IEEE Transactions on Medical Imaging*, 20(12):1251–1260, 2001.

7. S. Haker, S. Angenent, A. Tannenbaum, and R. Kikinis. Nondistorting flattening maps and the 3D visualization of colon CT images. *IEEE Transactions on Medical Imaging*, 19:665–670, Dec. 2000.
8. X. Han, C. Xu, and J. L. Prince. A topology preserving level set method for geometric deformable models. *IEEE Transactions on PAMI*, 25(6):755–768, 2003.
9. L. Hong, S. Muraki, A. Kaufman, D. Bartz, and T. He. Virtual voyage: interactive navigation in the human colon. *SIGGRAPH*, pages 27–34, 1997.
10. W. Hong, X. Gu, F. Qiu, M. Jin, and A. Kaufman. Conformal virtual colon flattening. *ACM Symposium on Solid and Physical Modeling*, pages 85–94, 2006.
11. W. Hong, F. Qiu, and A. Kaufman. A pipeline for computer aided polyp detection. *IEEE Transactions on Visualization and Computer Graphics*, 12(5):861-868, 2006.
12. C. D. Johnson and A. H. Dachman. CT colonography: The next colon screening examination? *Radiology*, 216(2):331–341, 2000.
13. G. Kiss, J. Cleynenbreugel, M. Thomeer, P. Suetens, and G. Marchal. Computer-aided diagnosis in virtual colonography via combination of surface normal and sphere fitting methods. *European Journal of Radiology*, 12:77–81, 2002.
14. J. Kruger and R. Westermann. Acceleration techniques for GPU-based volume rendering. *IEEE Visualization*, pages 38–44, 2003.
15. J. S. Mandel, J. H. Bond, T. R. Church, D. C. Snover, G. M. Bradley, L.M. Schuman, and F. Ederer. Reducing mortality from colorectal cancer by screening for fecal occult blood. *New England Journal of Medicine*, 328(19):1365–1371, 1993.
16. J. Nappi, H. Frimmel, A. Dachman, and H. Yoshida. Computerized detection of colorectal masses in ct colonography based on fuzzy merging and wall-thickening analysis. *Medical Physics*, 31:860–872, 2004.
17. J. Nappi and H. Yoshida. Feature-guided analysis for reduction of false positives in cad of polyps for CT colonography. *Medical Physics*, 30:1592–1601, 2003.
18. D. S. Paik, C. F. Beaulieu, G. D. Rubin, B. Acar, R. B. Jeffery, J. Yee, J. Dey, and S. Napel. Surface normal overlap: a computer-aided detection algorithm with application to colonic polyps and lung nodules in helical CT. *IEEE Transactions on Medical Imaging*, 23(6):661–675, June 2004.
19. P. J. Pickhardt, J. R. Choi, I. Hwang, J. A. Butler, M. L. Puckett, H. A. Hildebrandt, R. K. Wong, P. A. Nugent, P. A. Mysliwiec, and W. R. Schindler. Computed tomographic virtual colonoscopy to screen for colorectal neoplasia in asymptomatic adults. *The New England Journal of Medicine*, 349(23):2191–2200, Dec. 2003.
20. R. M. Summers, C. D. Johnson, L. M. Pusanik, J. D. Malley, A. M. Youssef, and J. E. Reed. Automated polyp detection at CT colonography: Feasibility assessment in a human population. *Radiology*, 219(1):51–59, 2001.
21. C. Tomasi and S. B. Göktürk. A graph method for the conservative detection of polyps in the colon. *Second International Symposium on Virtual Colonoscopy*, 2000.
22. D. Vining, Y. Ge, D. Ahn, and D. Stelts. Virtual colonoscopy with computer-assisted polyps detection. *Computer-Aided Diagnosis in Medical Imaging*, pages 445–452, 1999.
23. M. Wan, F. Dachille, K. Kreeger, S. Lakare, M. Sato, A. Kaufman, M. Wax, and J. Liang. Interactive electronic biopsy for 3D virtual colonoscopy. *SPIE Medical Imaging*, 4321:483–488, 2001.
24. G. Wang and M. W. Vannier. GI tract unraveling by spiral CT. *Proceedings SPIE*, 2434:307–315, 1995.
25. Z. Wang, Z. Liang, L. Li, X. Li, B. Li, J. Anderson, and D. Harrington. Reduction of false positives by internal features for polyp detection in CT-based virtual colonoscopy. *Medical Physics*, 32(12):3602–3616, 2005.
26. Z. Wang, Z. Liang, X. Li, L. Li, D. Eremina, and H. Lu. An improved electronic colon cleansing method for detection of colonic polyps by virtual colonoscopy. *IEEE Transactions on Biomedical Engineering*, 53:1635–1646, 2006.
27. J. Yao, M. Miller, M. Franaszek, and R. Summers. Colonic polyp segmentation in CT colonoscopy-based on fuzzy clustering and deformable models. *IEEE Transactions on Medical Imaging*, 23:1344–1352, 2004.
28. H. Yoshida, Y. Masutani, P. MacEneaney, D. T. Rubin, and A. H. Dachman. Computerized detection of colonic polyps in CT colonography based on volumetric features: A pilot study. *Radiology*, pages 327–336, Jan. 2002.
29. H. Yoshida and J. Näppi. Three-dimensional computer-aided diagnosis scheme for detection of colonic polyps. *IEEE Transactions on Medical Imaging*, 20(12):1261–1274, 2001.
30. N. Zhang, W. Hong, and A. Kaufman. Dual contouring with topology preserving simplification using enhanced cell representation. *IEEE Visualization*, pages 505–512, Oct. 2004.